Journal of the Korean Physical Society, Vol. 73, No. 10, November 2018, pp. 1577∼1583

Development of a Method for Improving the Electric Field Distribution in Patients Undergoing Tumor-Treating Fields Therapy

Jiwon Sung, Jaehyeon Seo, Yunhui Jo and Myonggeun Yoon*
Department of Bio-convergence Engineering, Korea University, Seoul 02841, Korea

Sang-Gu Hwang and Eun Ho Kim
Korea Institute of Radiological and Medical Sciences, Seoul 01812, Korea

(Received 30 April 2018, in final form 9 July 2018)

Tumor-treating fields therapy involves placing pads onto the patient's skin to create a low- intensity (1 - 3 V/cm), intermediate frequency (100 - 300 kHz), alternating electric field to treat cancerous tumors. This new treatment modality has been approved by the Food and Drug Administration in the USA to treat patients with both newly diagnosed and recurrent glioblastoma. To deliver the prescribed electric field intensity to the tumor while minimizing exposure of organs at risk, we developed an optimization method for the electric field distribution in the body and compared the electric field distribution in the body before and after application of this optimization algorithm. To determine the electric field distribution in the body before optimization, we applied the same electric potential to all pairs of electric pads located on opposite sides of models. We subsequently adjusted the intensity of the electric field to each pair of pads to optimize the electric field distribution in the body, resulting in the prescribed electric field intensity to the tumor while minimizing electric fields at organs at risk. A comparison of the electric field distribution within the body before and after optimization showed that application of the optimization algorithm delivered a therapeutically effective electric field to the tumor while minimizing the average and the maximum field strength applied to organs at risk. Use of this optimization algorithm when planning tumor-treating fields therapy should maintain or increase the intensity of the electric field applied to the tumor while minimizing the intensity of the electric field applied to organs at risk. This would enhance the effectiveness of tumor-treating fields therapy while reducing dangerous side effects.

PACS numbers: 87.85.−d, 87.55.ne, 87.55.de, 87.55.D−
Keywords: Tumor-treating fields, Alternating electric field, Optimization algorithm, Cancer therapy, Electric field calculation
DOI: 10.3938/jkps.73.1577

I. INTRODUCTION

Tumor-treating fields (TTFields) therapy is a novel antimitotic cancer treatment modality that disrupts cancer cell replication by applying alternating electric fields of low intensity (1 - 3 V/cm) and intermediate frequency (100 - 300 kHz) [1,2]. Because its efficacy in treating patients with recurrent glioblastoma (GBM) was comparable to that of chemotherapy, but with fewer side effects, TTFields therapy was approved by the U.S. Food and Drug Administration (FDA) in 2011 to treat patients with recurrent GBM. TTFields therapy in combination with chemotherapy was shown to enhance survival compared with chemotherapy alone in patients with newly diagnosed GBM, resulting in its approval by the FDA in 2015 for this indication [3–6]. At present, only six years after its initial approval by the U.S. FDA, TTFields therapy is being performed to treat GBM in about 950 treatment centers worldwide. Moreover, clinical trials have reported that TTFields therapy is 1.5 - 2.5 times more effective than conventional treatments in patients with lung, pancreatic and ovarian cancer, and it is being evaluated in other types of cancer [7–12].

Efforts are also underway to maximize the therapeutic effects of TTFields therapy. A previous study showed that the force exerted on a microscopic polarizable organelle in the cell is proportional to the square of the electric field, *i.e.*, the electric field intensity [13]. As a result, increases in the electric field intensity have been found to result in greater blockage of cancer cell division and induction of cell death in various cancer cell lines [13–16]. Specific frequency ranges have shown maximum effectiveness at blocking cancer cell division, even at the same electric field intensity [2, 13, 15]. Electric fields of about 200 kHz have shown the maximum effect

*E-mail: radioyoon@korea.ac.kr; Fax: +82-2-940-2829

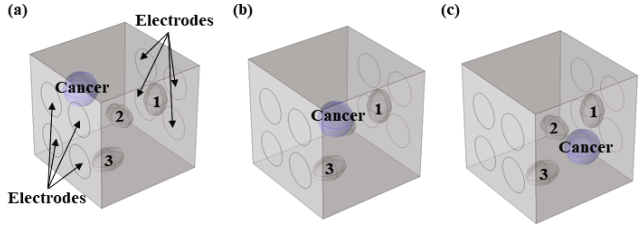

Fig. 1. (Color online) Simple Model Structure.

in treating patients with GBM, and the TTFields treatment planning system, NovoTAL software, determines the size and the position of the tumor relative to each patient's individual anatomy and selects the position of the electric pads to maximize the field strength at the tumor during treatment [17–19].

Although TTFields treatment is a promising modality to treat patients with various types of cancers, it has the potential for long-term side effects. It is, therefore, important to study methods that increase the intensity of electric fields applied to tumors, thereby enhancing its the therapeutic effects, while minimizing exposure of organs at risk (OARs). Few studies, however, have assessed methods for optimizing the intensities of electric field [20,21]. Optimization algorithms that control the amount of radiation administered are frequently used for patients undergoing conventional radiation therapy [22–24]. These algorithms are based on determinations of the prescribed dose to be applied to the tumor and the allowable dose to OARs that does not cause side effects. This method can more easily control radiation dose to the body than methods in which several conditions (*e.g.*, the amount, direction, and intensity of radiation) are repeatedly changed, requiring re-calculation of radiation doses delivered to the body [25–27].

Similar to planning methods for radiotherapy, we used an optimization algorithm to optimize the electric field distribution in the body, allowing the application of electric fields with the prescribed intensities to tumors while minimizing the intensities of electric fields at OARs. The distributions of the electric fields in the body were compared using this method and existing treatment approaches that do not use optimization algorithms.

II. EXPERIMENTS

1. Design of model

This research was performed using simple self-made models and models based on actual patients' computed tomography (CT) dicom files. The simple model consisted of an 8000-cm^3 cube containing three ovals, each 50.1 cm^3 in volume but at different positions, as well as one 112.5 cm^3 sphere; these represented OARs 1, 2, and 3 and the tumor, respectively (Fig. 1). Three types of

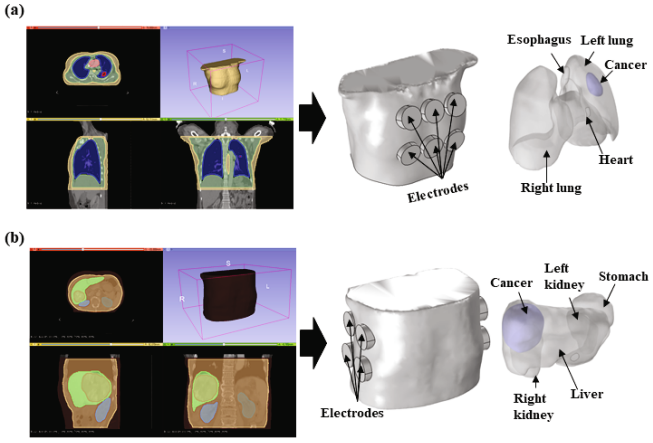

Fig. 2. (Color online) Interior and exterior of the patient model created based on CT data for patients with (a) lung and (b) liver cancer.

models were constructed, differing only in the position of the tumor, which was at the top (Fig. 1(a)), center (Fig. 1(b)), or bottom (Fig. 1(c)) of the cube. The area of each electrode that transmit the electric field to the model was 28.3 cm^2. Four electrodes are attached to each of the two opposite sides of the cube, with a 2-cm gap between electrodes.

Patient models were based on the CT dicom files of actual patients with lung and liver cancer. In the lung cancer model, OARs, such as the lungs, esophagus, and heart, were segmented based on CT images, and the tumor was drawn on the CT images. In the liver cancer model, OARs, such as the stomach and kidneys, as well as the tumors, were segmented based on CT images. Volume meshes were made via simpleware software (Synopsys, USA) and were transferred to COMSOL Multiphysics software (COMSOL, USA). The lung cancer model included six electrodes, of around 28.5 cm^2, placed in the area of each of the two opposite skin surfaces whereas the liver cancer model included four electrodes, of around 30.6 cm^2, in the area of each of the two opposite skin surfaces (Fig. 2).

2. Computation of electric fields

The electric fields formed within the models were calculated using the COMSOL AC/DC module, which performs a finite-element analysis of Maxwell's equations. In the simple models, the conductivity of all organs was set at 0.1 S/m, and the permittivity was set at 1000. In the patient models, the conductivity and the permittivity values at 200 kHz were set to values appropriate for each organ from the literature [20,28,29]. Electrodes on the two opposing sides were selected one by one so that all the electrodes on one side could be matched with those on the other side one by one. To calculate the electric

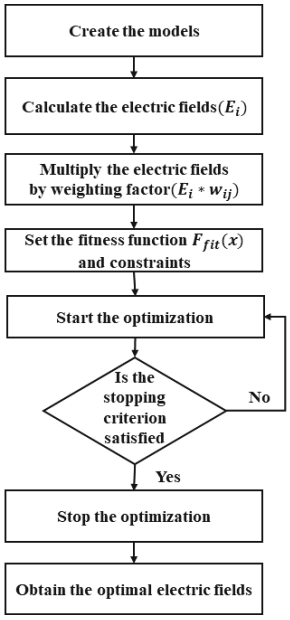

Fig. 3. Process for calculating the optimal electric field distribution through the optimization algorithm.

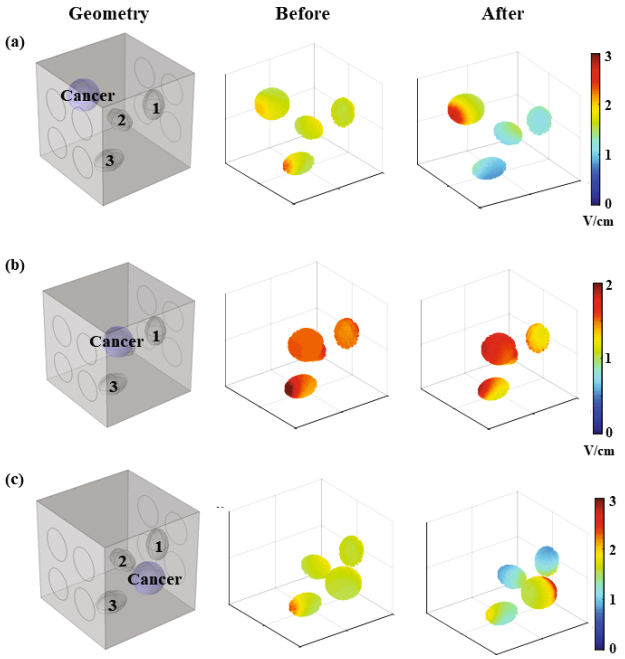

Fig. 4. (Color online) Interior electric-field distributions before and after application of the optimization algorithm for tumors located at the (a)top, (b)center, and (c)bottom of the cube.

field, we set the alternating current (AC) voltage of one electrode was to 10 - 100 V_{pp}, 200 kHz and the corresponding electrode at ground. That is, 16 ($E_1 \sim E_{16}$) and 36 ($E_1 \sim E_{36}$) electric field distributions were obtained for models with four and six electrodes on each side, respectively. These electric field distribution values (E_i) were each multiplied by weighting factors (w_i), and the final distribution (E_{fianl}) was calculated by the combination of these distribution values, as in Eq. (1).

$$E_{\text{fianl}}(w_{ij}) = \frac{\sum_{i=1}^{n} w_{ij} * E_i}{\text{Number of electrodes used}}. \quad (1)$$

3. Optimization method

This research used a genetic algorithm (GA), a global optimization algorithm technique based on Darwin's concept of survival of the fittest [30,31]. A randomly created initial population is subjected to three processes (selection, crossover, and mutation) based on the resulting values of a calculated fitness function, to create a population that is more evolved than the initial population. The genetic processes are performed again based on this population's resulting values to create another population, and the process is repeated. When set conditions are met or a better fitness function cannot be obtained, the algorithm is considered to have found the optimal condition (Fig. 3) [31–33].

Equation (2) was set as the fitness function, and optimization was performed to adjust the weighting factors to obtain the minimum fitness function value (F_{fit}). If E_{ave1}, E_{ave2}, and E_{ave3} are the mean electric field values transmitted to the OARs, and Std_{cancer} is the standard deviation of the electric field intensity transmitted to the tumor, then

$$F_{\text{fit}}(w_{ij}) = E_{\text{ave1}}(w_{ij}) + E_{\text{ave2}}(w_{ij}) + E_{\text{ave3}}(w_{ij}) + Std_{\text{cancer}}(w_{ij}). \quad (2)$$

Constraints were designed to deliver an electric field strength $\geq$ 1.5 V/cm to the tumor and less than the maximum field strength to the OARs when the same electric potential was applied to all electrodes.

4. Evaluation method

To evaluate the treatment planning method using the optimization algorithm, we determined the electric field distribution in the body resulting from the application of the same electric potential to all the electrodes on opposite sides. These findings were normalized to allow transmission of an electric field $>$ 1.5 V/cm to the entire volume of the tumor.

The two methods were evaluated by constructing a 3-D map representing the electric field intensity transmitted to the tumor and the OARs (Figs. 4 and 6) and by constructing a graph in which the horizontal axis represent the electric field intensity and the vertical axis represent the percentage of the total volume of a given tissue in which the magnitude of the electric field exceeded that

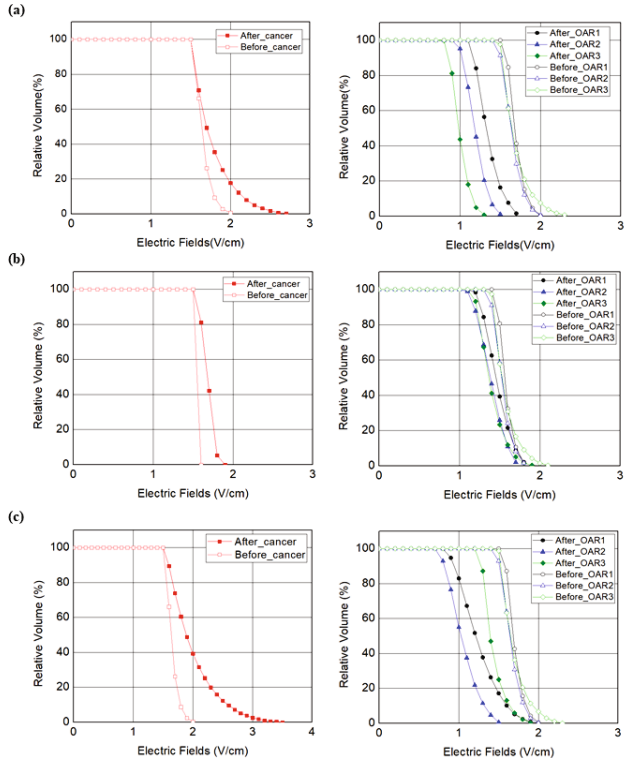

Fig. 5. (Color online) Percentage of the total volume of a given tissue in which the magnitude of the electric field exceeded that along the horizontal axis before and after application of the optimization algorithm for tumors located at the (a) top, (b) center, and (c) bottom of the cube.

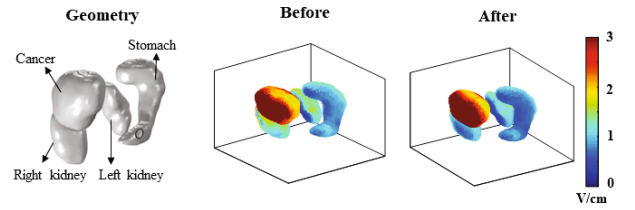

Fig. 6. (Color online) Distributions of internal electric fields in a liver cancer model before and after application of the optimization algorithm.

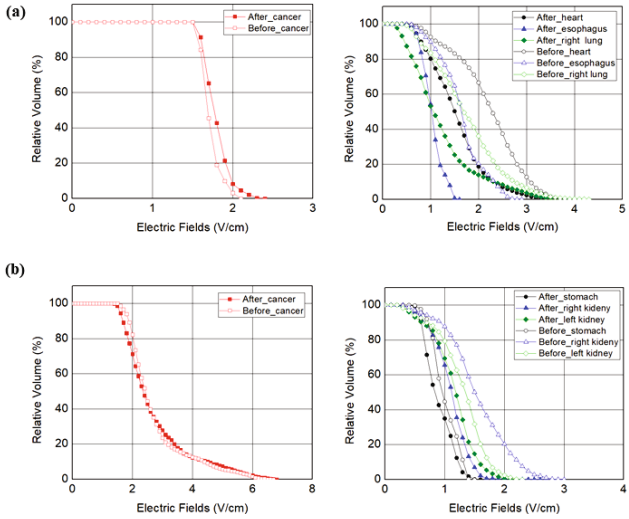

Fig. 7. (Color online) Percentage of the total volume of a given tissue in which the magnitude of the electric field exceeded that along the horizontal axis before and after application of the optimization algorithm in the (a) lung and (b) liver cancer models.

in the horizontal axis in V/cm (Figs. 5 and 7), the maximum electric field intensity of the specific organ ($E_{\max}$), the average electric field intensity of the specific organ (E_{ave}), and the values (V_{30}, V_{60}, V_{90}) of the relative volume which had 30% (= 0.45 V/cm), 60% (= 0.90 V/cm), or 90% (= 1.35 V/cm) of 1.5 V/cm transmitted. These factors are those used for evaluating radiation treatment plans [34,35].

III. RESULTS AND DISCUSSION

1. Simple models

Figure 4 shows 3-D graphs of the internal electric field distributions with (optimization method) and without (existing method) the optimization algorithm, enabling a qualitative determination of the electric field intensity transmitted to each internal organ. In all three models, there were more areas of application of $\geq$ 2 V/cm electric field intensity to the tumor than in the existing method, along with many areas of application of $\leq$ 1 V/cm electric-field intensity at the OARs. A comparison of the two methods in Fig. 4(a) showed that the optimization method increased the area of the tumor exposed to $\geq$ 2 V/cm by more than half and reduced the intensity to most OARs from 1 - 1.5 V/cm to $<$ 1 V/cm. In Fig. 4(b), the optimization method increased the intensity to most of the tumor to $\geq$ 2 V/cm and altered the intensity to most OARs from 1.5 - 2 V/cm to around 1 V/cm. In Fig. 4(c), the optimization method increased the area of the tumor exposed to 2 V/cm by around half and reduced exposure of about half of the OARs from 1.5 - 2 V/cm to $<$ 1 V/cm. Also, regardless of whether the existing method or the optimization method was used, the electric fields were greater in some parts of the tumor than in other parts and were greater for OARs near the surface than for OARs at deeper locations. This was likely due to the greater electric field intensity in areas close to, rather than more removed from, an electrode, thereby increasing exposure of organs near surface electrodes.

The treatment plan was designed so that the entire volume was exposed to an electric field $\geq$ 1.5 V/cm (Fig. 5). The maximum electric-field intensity transmitted to the tumor was larger after than before using the optimization algorithm (2.77 V/cm vs. 2.40 V/cm, respectively,

Table 1. Comparisons of the V_{30}, V_{60}, V_{90}, $E_{\max}$, and E_{ave} values for each OAR for tumors at the (a) top, (b) center, and (c) bottom of the cube.

(a)	Organ 1			Organ 2			Organ 3		
	BO	AO	Difference	BO	AO	Difference	BO	AO	Difference
V_{30}	100	100	0	100	100	0	100	100	0
V_{60}	100	100	0	100	100	0	100	81	19
V_{90}	100	44	56	100	13	87	100	0	100
$E_{\max}$	2.02	1.78	0.24	2.02	1.53	0.49	2.40	1.34	1.06
E_{ave}	1.70	1.35	0.35	1.65	1.19	0.46	1.69	1.00	0.69
(b)	Organ 1			Organ 2			Organ 3		
	BO	AO	Difference	BO	AO	Difference	BO	AO	Difference
V_{30}	100	100	0	100	100	0	100	100	0
V_{60}	100	100	0	100	100	0	100	100	0
V_{90}	100	74	26	99	58	41	100	53	47
$E_{\max}$	1.88	1.87	0.01	1.88	1.78	0.10	2.19	1.93	0.26
E_{ave}	1.58	1.47	0.11	1.53	1.39	0.14	1.57	1.39	0.18
(c)	Organ 1			Organ 2			Organ 3		
	BO	AO	Difference	BO	AO	Difference	BO	AO	Difference
V_{30}	100	100	0	100	100	0	100	100	0
V_{60}	100	95	5	100	77	23	100	100	0
V_{90}	100	32	68	100	8	92	100	67	33
$E_{\max}$	2.03	2.03	0.00	2.02	1.59	0.43	2.36	1.96	0.40
E_{ave}	1.70	1.25	0.45	1.65	1.05	0.60	1.69	1.43	0.26

Abbreviations: BO, before application of the optimization algorithm; AO, after application of the optimization algorithm.

Table 2. Comparison of the V_{30}, V_{60}, V_{90}, $E_{\max}$, and E_{ave} values for each OAR in the (a) lung and (b) liver cancer models.

(a)	Heart			Esophagus			Right Lung		
	BO	AO	Difference	BO	AO	Difference	BO	AO	Difference
V_{30}	100	100	0	100	100	0	100	90	10
V_{60}	96	85	11	93	71	22	86	61	25
V_{90}	89	61	28	74	12	62	68	34	34
$E_{\max}$	4.11	3.58	0.53	2.81	1.53	1.28	4.36	4.00	0.36
E_{ave}	2.22	1.54	0.68	1.63	1.03	0.60	1.76	1.23	0.53
(b)	Stomach			Right Kidney			Left Kidney		
	BO	AO	Difference	BO	AO	Difference	BO	AO	Difference
V_{30}	100	100	0	98	97	1	95	95	0
V_{60}	58	43	15	91	76	15	85	78	7
V_{90}	5	3	2	65	19	46	50	27	23
$E_{\max}$	1.44	1.52	-0.08	2.98	2.85	0.13	2.23	2.13	0.10
E_{ave}	0.99	0.89	0.10	1.55	1.09	0.46	1.29	1.15	0.14

Abbreviations: BO, before application of the optimization algorithm; AO, after application of the optimization algorithm.

in Fig. 5(a); 1.88 V/cm vs. 1.55 V/cm, respectively, in Fig. 5(b); and 3.54 V/cm vs. 2.05 V/cm, respectively, in Fig. 5(c)). The optimization method resulted in the transmission of 0.33 - 1.49 V/cm greater intensity. These findings confirmed that the optimization algorithm made possible the application of a greater electric field to the tumor than the existing method.

In assessing OAR graphs (Fig. 5), we found that all the graphs for the optimization method were positioned to the left (y-axis) of the graphs for the existing method, with the optimization method having a similar or lower maximum electric-field intensity. Quantitative analyses also showed that the maximum electric-field intensity was equal or lower using the optimization than the existing method in all three organs at risk in all three models (*i.e.* nine conditions), with differences of 0.00 - 1.06 V/cm (Table 1). The average electric-field intensity was also lower in all nine conditions, with differences of 0.11 - 0.69 V/cm. Comparing the electric-field intensity doses in sections showed that the relative volumes of OARs exposed to 0.45 V/cm (V_{30}) were 100%. Compared with the existing method, use of the optimization method reduced the volume exposed to 0.90 V/cm (V_{60}) by 5% - 23% in three of the nine conditions and reduced the volume exposed to 1.35 V/cm (V_{90}) by 26% - 100% under all nine conditions. That is, the higher the electric field strength is the smaller the volume of normal tissue exposed.

Figure 6 shows the 3-D electric field distribution when an electric field is applied to a CT image-based liver cancer patient model using the existing treatment method and the optimization algorithm to create treatment plans. The differences in the electric-field intensity were not as obvious as in the simple model, although the use of the optimization algorithm increased the volume of the tumor exposed to 3 V/cm slightly, and reduced the volume of the right kidney exposed to 1 - 2 V/cm, with these areas being exposed to electric-field intensity < 1 V/cm. Use of the optimization algorithm also increased the volume of the stomach exposed to < 0.5 V/cm.

Although the overall shapes of the tumor graphs were similar for the existing and the optimization methods (Fig. 7), the maximum electric-field intensities transmitted to the tumor using these two methods were 2.09 V/cm and 2.35 V/cm, respectively, for the lung cancer model (Table 2(a)) and 6.62 V/cm and 6.72 V/cm, respectively, for the liver cancer model (Table 2(b)). The greater maximum electric-field intensity in the liver model compared to the lung cancer model was likely due to the greater electric-field intensity in areas around the electrode. Because liver tumors are closer to the electrode than lung tumors, the maximum electric-field intensity at the former should be higher.

When we compared each of the OARs, we found that the graph lines of the optimization method were generally to the left (y-axis) of the graph lines of the existing method (Fig. 7). That is, the electric-field intensity transmitted to each OAR was lower by the optimization method than by the existing method. Quantitative analysis also showed that the maximum electric-field intensity was lower for the optimization than for the existing method for all six OARs in both the lung (Table 2(a)) and the liver (Table 2(b)) cancer models, except for the stomach, with differences ranging from 0.10 - 1.28 V/cm. Although the maximum electric-field intensity for the stomach was greater for the optimization than for the existing method, the difference, 0.08 V/cm, was very small. Similarly, comparisons of average electric-field in-

tensities showed that the intensities transmitted to all six OARs was 0.10 - 0.68 V/cm lower with the optimization method.

Assessment of the relative volume of each organ that experienced each level of electric-field intensity showed that the relative volume that experienced more than 0.45 V/cm (V_{30}) was the same for four of the six OARs, but in two of them the optimization method affected a smaller volume. The relative volume exposed to 0.90 V/cm (V_{60}) was 7% - 25% smaller with the optimization method than the existing method for all six OARs. Moreover, the relative volume exposed to 1.35 V/cm (V_{90}) was 2% - 62% smaller with the optimization method for all six OARs. Thus, similar to the simple model, the volume of normal tissue that experienced high levels of electric-field intensity was lower when the optimization method was used.

When an optimization algorithm is used, large and small electrical potentials are generally applied to the electrode near the tumor and the electrode near the OARs, respectively. Therefore, if optimization is used, local electric field intensities applied to the patient's skin below the electrodes can be relatively large or small based on the locations of the electrodes. However, the averages of the electric field intensity applied to the entire skin stayed the same before and after optimization. Our experimental results showed that average electric fields applied to the skin before and after optimization were 0.82 V/cm (0.59 V/cm) per unit skin area and 0.73 V/cm (0.4 V/cm) per unit skin area for the liver (lung), respectively. Although electrode induced local electric fields applied to patient's skin can be relatively large causing skin side effect, this phenomenon can be avoided if the limit of electric field is applied during optimization.

In addition to intensity modulation of the TTFields, one can adjust the electrode size to optimize the electric field inside body. In general, when a small electrode is used, there are several advantages. First, there will be more electrodes (*i.e.*, variables) that can be manipulated to focus the electric field inside body. Second, small electrode can be easily attached to the skin, which is very important issue in TTF therapy. However, if one uses only small electrodes, the high electric field acquired by optimization can be applied to a very small area just below the specific electrode, which might cause a side effect in the skin. On the other hand, when a large electrode is used, it is an advantage to apply a uniform electric field in the body with relatively small electric field on the skin. But, as mentioned before, it might be difficult for large electrode to be attached to the patient's skin completely. Therefore, the appropriate sizes of electrodes are very important in optimization of electric field using intensity modulation and future study is called to investigate the optimal electrode size and field intensity for the best outcome of tumor treating fields.

IV. CONCLUSION

This study compared the electric-field distributions in the body produced using an optimization algorithm and an existing treatment method. The optimization method resulted in application of a greater electric-field intensity to the tumor while minimizing the electric field intensity at OARs. Use of this method in actual treatment plans may not only increase the effectiveness of the treatment, but also reduce as yet undetermined side effects of TTFields therapy. In the future, we will study the difference in the electric field distribution due to the different electric susceptibilities of organs and prostheses to improve the effect of TTFields therapy.

ACKNOWLEDGMENTS

This work was supported by a National Research Foundation of Korea (NRF) grant (NRF-2015M2A2A7A02045273, NRF-2017M2A2A7081416, NRF-2018R1D1A1B07047770) funded by the Korean government.

REFERENCES

[1] A. M. Davies, U. Weinberg and Y. Palti, Ann. Ny. Acad. Sci. **1291**, 86 (2013).
[2] M. Pless and U. Weinberg, Expert Opin. Inv. Drug **20**, 1099 (2011).
[3] S. Kesari, Z. Ram and E. F. T. Investigators, CNS Oncol. **6**, 185 (2017).
[4] E. H. Kim, Y. J. Kim, H. S. Song, Y. K. Jeong, J. Y. Lee, J. Sung, S. H. Yoo and M. Yoon, Oncotarget **7**, 62267 (2016).
[5] R. Stupp *et al.*, Jama-J. Am. Med. Assoc. **314**, 2535 (2015).
[6] C. Wenger, Z. Bomzon, R. Salvador, P. J. Basser and P. C. Miranda, Conf. Proc. IEEE Eng. Med. Biol. Soc. **2016**, 5664 (2016).
[7] F. Rivera, J. Gallego, C. Guillen, M. Benavides, J. A. Lopez-Martin and M. Kueng, J. Clin. Oncol. **34**, 269 (2016).
[8] M. Pless, C. Droege, R. von Moos, M. Salzberg and D. Betticher, Lung Cancer **81**, 445 (2013).
[9] N. Hanna *et al.*, J. Clin. Oncol. **22**, 1589 (2004).
[10] D. D. Von Hoff *et al.*, New. Engl. J. Med. **369**, 1691 (2013).
[11] I. Vergote, R. von Moos, L. Manso and C. Sessa, J. Clin. Oncol. **35**, 5580 (2017).
[12] A. M. Poveda, F. Selle, F. Hilpert, A. Reuss, A. Savarese, I. Vergote, P. Witteveen, A. Bamias, N. Scotto, L. Mitchell and E. Pujade-Lauraine, J. Clin. Oncol. **33**, 3836 (2015).
[13] E. D. Kirson, Z. Gurvich, R. Schneiderman, E. Dekel, A. Itzhaki, Y. Wasserman, R. Schatzberger and Y. Palti, Cancer Res. **64**, 3288 (2004).

[14] M. Silginer, M. Weller, R. Stupp and P. Roth, Cell Death Dis. **8**, e2753 (2017).
[15] E. D. Kirson *et al.*, P. Natl. Acad. Sci. USA **104**, 10152 (2007).
[16] H. Jeong, J. Sung, S. I. Oh, S. Jeong, E. K. Koh, S. Hong and M. Yoon, Appl. Phys. Lett. **105**, 203703 (2014).
[17] A. Chaudhry, L. Benson, M. Varshaver, O. Farber, U. Weinberg, E. Kirson and Y. Palti, World J. Surg. Oncol. **13**, 316 (2015).
[18] J. Connelly, A. Hormigo, N. Mohilie, J. Hu, A. Chaudhry and N. Blondin, Bmc Cancer **16**, 842 (2016).
[19] P. C. Miranda, A. Mekonnen, R. Salvador and P. J. Basser, Phys. Med. Biol. **59**, 4137 (2014).
[20] C. Wenger, R. Salvador, P. J. Basser and P. C. Miranda, Int. J. Radiat. Oncol. **94**, 1137 (2016).
[21] M. Macedo, C. Wenger, R. Salvador, S. R. Fernandes and P. C. Miranda, Conf. Proc. IEEE Eng. Med. Biol. Soc. **2016**, 5168 (2016).
[22] Q. W. Wu and R. Mohan, Med. Phys. **27**, 701 (2000).
[23] X. D. Zhang, H. Liu, X. C. Wang, L. Dong, Q. W. Wu and R. Mohan, Med. Phys. **31**, 1141 (2004).
[24] K. H. Chang, S. Lee, Y. J. Cao, J. B. Shim, J. E. Lee, J. A. Lee, D. S. Yang, Y. J. Park, W. S. Yoon, C. Y. Kim, S. J. Cho, S. H. Lee, W. C. Kim, C. K. Min, K. H. Cho and H. D. Huh, J. Korean Phys. Soc. **64**, 1047 (2014).
[25] L. Fenkell, I. Kaminsky, S. Breen, S. Huang, M. Van Prooijen and J. Ringash, Radiother. Oncol. **89**, 287 (2008).
[26] L. K. Schubert, V. Gondi, E. Sengbusch, D. C. Westerly, E. T. Soisson, B. R. Paliwal, T. R. Mackie, M. P. Mehta, R. R. Patel, W. A. Tome and G. M. Cannon, Radiother. Oncol. **100**, 241 (2011).
[27] A. Michalski, J. Atyeo, J. Cox, M. Rinks, M. Morgia and G. Lamoury, Med. Dosim. **39**, 163 (2014).
[28] C. Gabriel, AL/OE-TR-1996-0004 (1996).
[29] C. Gabriel, S. Gabriel and E. Corthout, Phys. Med. Biol. **41**, 2231 (1996).
[30] M. Gen and R. Cheng, *Genetic algorithms and engineering optimization* (John Wiley & Sons, 2000), Vol. 7.
[31] Y. J. Li, D. Z. Yao, J. Yao and W. F. Chen, Phys. Med. Biol. **50**, 3491 (2005).
[32] X. Wu and Y. Zhu, Phys. Med. Biol. **46**, 1085 (2001).
[33] J. Bang and S. Yoo, J. Korean Phys. Soc. **65**, 2001 (2014).
[34] M. Peszynska-Piorun, J. Malicki and W. Golusinski, Radiol. Oncol. **46**, 328 (2012).
[35] E. K. Koh, J. Seo, T. S. Baek, E. J. Chung, M. Yoon and H. H. Lee, J. Korean Phys. Soc. **63**, 97 (2013).